SECED 2023 Conference
Earthquake Engineering & Dynamics for a Sustainable Future
14-15 September 2023, Cambridge, UK

SEISMIC DESIGN OF AN INNOVATIVE SELF-CENTRING HYBRID COUPLED WALL SYSTEM: AN EIGHT-STORY CASE STUDY BUILDING

Mojtaba FARAHI[1], Fabio FREDDI[2] & Massimo LATOUR[3]

Abstract: *Several innovative solutions have been proposed over the last few decades to improve the seismic resilience of building structures. Most of these solutions aim to concentrate the damage in a few components and reduce residual deformations, thus expediting the repair time and operations in the aftermath of a damaging event. This paper presents the design and investigates the seismic performance of an innovative hybrid wall system consisting of a reinforced concrete (RC) wall coupled with two steel side columns. In this system, the coupling beams are integrated with friction-damped self-centring links, which dissipate the seismic energy while also limiting the residual deformations. The coupling action in the side steel columns also reduces the flexural demand at the wall base under lateral loading. The efficiency of a simple design methodology is investigated by targeting the concentration of non-linear deformations and energy dissipation in the self-centring links, hence limiting the damage to the RC wall. An eight-story case study structure is selected to perform a parametric analysis on the key design parameters of the self-centring hybrid wall (SCHW) structure and to investigate their influence on the seismic response. Detailed finite element models are developed in OpenSees to perform non-linear static and time-history analyses. The results inform on the validity of the design method and provide insights into the optimal choice of the key design parameters.*

Introduction

Reinforced concrete (RC) coupled walls are commonly used as lateral load-resisting systems for medium- to high-rise buildings in seismic-prone regions thanks to their superior strength and stiffness (Shahrooz et al., 1993, El-Tawil et al., 2010). However, their performance could be undermined by large residual deformations due to the significant damage that is typically experienced by the coupling beams during severe earthquakes (Wallace et al., 2012, Kam and Pampanin, 2011, Wang, 2008, Westenenk et al., 2012). Large earthquake-induced damages and residual deformations prevent the building from being easily and quickly repaired and lead to significant direct (*e.g.,* repair cost) and indirect (*e.g.,* downtime) socioeconomic losses. This foregrounds the eminent need for 'seismic-resilient' structural solutions providing ductility and energy dissipation capacity in conjunction with self-centring (SC) capability facilitating structural repairs after severe earthquakes.

To improve the ductility and energy dissipation capacity of coupled systems, Zona *et al.* proposed an innovative steel and concrete hybrid structural solution (Zona et al., 2016, Das et al., 2018) named Hybrid Coupled Wall (HCW). In HCWs, a central RC wall is coupled to two side steel columns with replaceable steel links pinned to the columns. Damaged links are supposed to be replaced after severe ground motions. However, the practicality of replacing damaged links can be challenging due to significant residual deformations expected after strong earthquakes.

An effective approach to mitigate the challenges posed by residual deformations is through the use of SC coupling beams. Several configurations of SC coupling beams, incorporating post-tensioned bars/cables, have been proposed to exploit their benefits (Ricles et al., 2002, Weldon and Kurama, 2010, Zareian et al., 2020). Typically, these configurations allow for a gap to open at the beam-to-wall interfaces, which is subsequently closed after loading, thanks to the restoring force provided by the post-tensioned bars/cables. Nevertheless, beam elongation under large

[1] Marie Curie Postdoctoral Fellow, University College of London, London, UK, mojtaba.farahi@ucl.ac.uk
[2] Lecturer, University College of London, London, UK
[3] Associate Professor, University of Salerno, Salerno, Italy

deformations can adversely affect the performance of these SC coupling beams (Deng et al., 2016).

This paper summarises a preliminary numerical study in which the seismic performance of an alternative structural system is investigated. This innovative system was inspired by the HCW system proposed by Zona *et al.* (2016) and features SC links in the coupling beams. The proposed lateral load-resisting system is referred to as Self-centring Hybrid Wall (SCHWs). A friction-damped SC link similar to the one proposed by Huang and Wang (2021) is adopted within the coupling beams in SCHWs. In addition to the typical benefits of SC connections (*i.e.,* controlled energy dissipation capacity, self-centring capability, and easy reparability), the proposed solution is also characterized by the following key advantages: (*1)* eliminates problems related to the coupling beams elongation; (*2)* allows the application of prefabricated SC components, which can resolve the issues caused by on-site post-tensioning. The proposed SCHWs and SC links are first discussed in this paper. A design framework is next introduced to design three case study SCHWs as lateral load-resisting systems of an eight-story building. The efficiency of the design procedure and the seismic performance of the SCHWs are eventually investigated through nonlinear static and dynamic analyses. The results highlight the advantages of the SCHWs as an alternative to seismic-resisting structural systems.

Hybrid coupled wall system and self-centering links

Figure 1 shows the hybrid lateral load-resisting system of interest composed of a central RC wall and two steel side columns connected by steel coupling beams. The coupling beams consist of three components; two side elements that are designed to remain elastic and a central SC link. One side element is protruded from the RC wall, and the other one is pinned to the side columns. Figure 1(a) represents the lateral load-resisting mechanism of SCHWs. It should be noted that the contribution of the steel columns in resisting lateral loads will be negligible and the columns shear force is ignored and not shown in this figure. In addition, the axial force that may develop in the RC wall due to random eccentricities is also assumed negligible. The coupling bending moment ($M_c = N_c \cdot L_{tot}$) contributes to resist the overall overturning moment due to lateral loading and reduces the bending moment demand at the base of the RC wall (M_w). The axial force developed in steel columns (N_c) is referred as the coupling action. It is distributed as the shear force demand in coupling beams at different stories. The ratio of the bending moment resisted by the side columns (M_c) to the total resisted bending moment ($M_c + M_w$) is called Coupling Ratio (CR) which is a key parameter in the design of coupled walls.

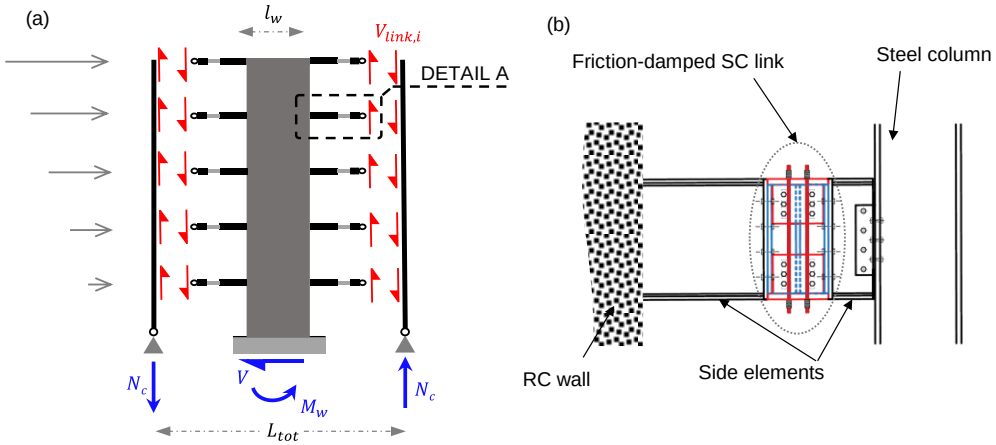

Figure 1. (a) Lateral load resisting mechanism in SCHWs, (b) Details of coupling beams in SCHWs.

The SC mechanism in the coupling beams is provided by a friction-damped SC link similar to the one proposed by Huang and Wang (2021). In the SC links adopted in this study, vertical PT bars provide the restoring force, and a friction slip mechanism provides the energy dissipation capacity. The SC links are composed of two restrainers (Figure 2(a)) and two identical T-shaped pieces (Figure 2(b)), which are fixed to the adjacent side elements. The restrainers are fabricated by welding one end of two frictional plates to an anchorage (horizontal) plate. Four PT bars are used to clamp the top and bottom restrainers to the T-shaped pieces, as depicted in Figure 2, and maintain the integrity of the SC links. The friction force and energy dissipation capacity of the SC

links are determined by the number of bolts passing through the frictional plates and the web of T-shaped pieces, the post-tensioning force in the bolts, and the friction coefficient at the interface. The oversized longitudinal slots in the web of T-shaped pieces (Figure 2(b)) should provide enough room for relative vertical movements at both ends. Hence, a double shear-frictional mechanism (top and bottom of the link) is activated once the shear force in the SC links exceeds the post-tension force in the PT bars.

Figure 2(c) schematically represents the flag-shaped shear force-chord rotation ($V_l - \gamma^{sl}$) behaviour expected for the intended SC link. Once the shear force in the SC link (V_l) exceeds the post-tensioning force in the PT bars (F_{PT}) and the frictional resistance between the web of T-shaped pieces and the frictional plates (F_{fr}), a gap is opened between the anchorage plates and the T-shaped pieces at opposite corners of the SC link (Figure 2(d)). The shear force at the onset of gap opening is referred to as the activation force ($F_{act} = F_{fr} + F_{PT}$) in this study. The stiffness of the SC link when the gap is open (K_{eq}) is calculated as a function of the stiffness of PT bars and disk springs. As the loading is reversed, the resistance frictional force developed due to the plates' slippage in the reverse direction shall also be overcame. After the frictional resistance is overcome, unloading is continued with a stiffness equal to K_{eq} until the gap is closed and the inelastic deformation is restored (Figure 2(c)).

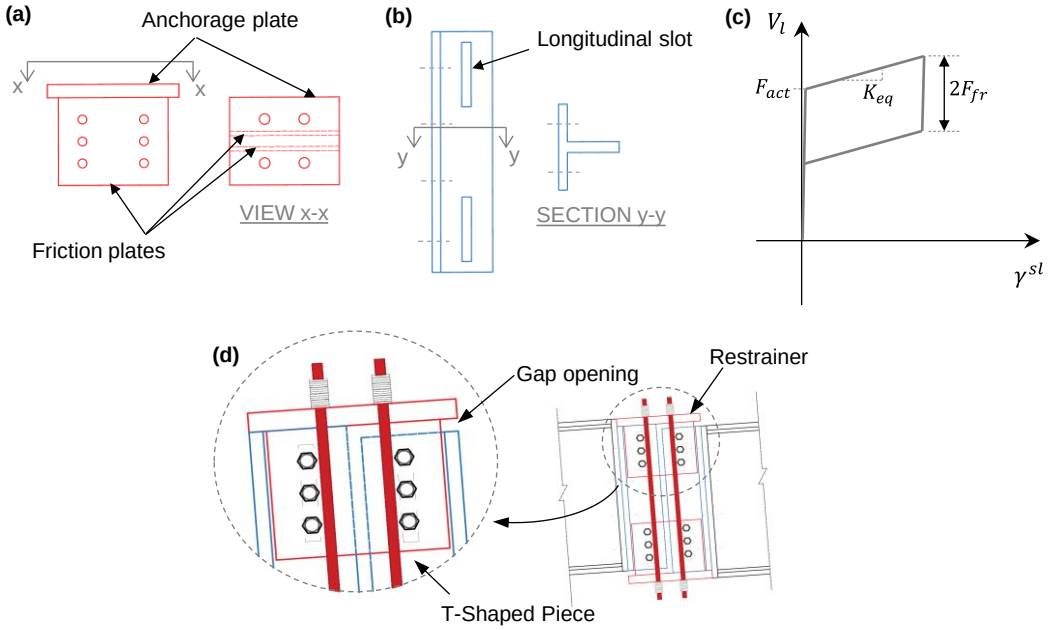

Figure 2. (a) Detail of SC links restrainer, (b) Detail of SC links T-shaped pieces, (c) Flag-shaped shear force-chord rotation response of SC links, (d) Vertical sliding mechanism in SC links.

Design of case study SCHWs

The case study SCHWs considered in this research are assumed to form the lateral load-resisting system of an eight-story building with plan and elevation shown in Figure 3. The lateral loading imposed on this building in each direction is supposed to be resisted by four identical SCHWs. Distributed dead and live gravity loads on each floor of the building were considered equal to 4.5, and 2 kN/m^2, respectively.

A height to width (h/l_w) ratio of 10 has been recommended for RC walls in coupled systems in previous studies (Zona et al., 2015) to limit the excessive lateral deformations while providing enough flexibility for the wall to allow plastic deformation in steel links. Considering this limit, two widths of $l_w = 3.2\ m$ and $l_w = 2.5\ m$ were chosen for case study SCHWs. The thickness of walls with 3.2 m and 2.5 m width was assumed equal to 400 and 350 mm, respectively. To start the design procedure, CR was set equal to 55% and 70% for the case study SCHWs with $l_w = 3.2\ m$ and $l_w = 2.5\ m$, respectively. Other components of the case study SCHWs were designed and sized to resist a base shear consistent with the equivalent design earthquake force

determined for coupled walls in accordance with the Eurocode 8 (2004). The behaviour factor was assumed q=5.4 according to the provisions of the Eurocode 8 for coupled wall systems in DCH. The equivalent design earthquake force was then calculated equal to 1000kN considering the Type 1 elastic response spectrum with a peak ground acceleration of 0.35g, soil type C, and a building's importance factor of 1.

Malla and Wijeyewickrema (2021) has recently developed a direct displacement-based design (DDBD) method for coupled walls, which was adopted in this study to assess the displacement capacity of the case study SCHWs. In this method, the multi-degree-of-freedom (MDOF) system of interest is converted to an equivalent single-degree-of-freedom (SDOF) system to simplify the estimation of seismic demands. The energy dissipation due to inelastic deformations of the structure is also considered by using inelastic acceleration/displacement demand spectra considering the ductility estimated for the system in this approach.

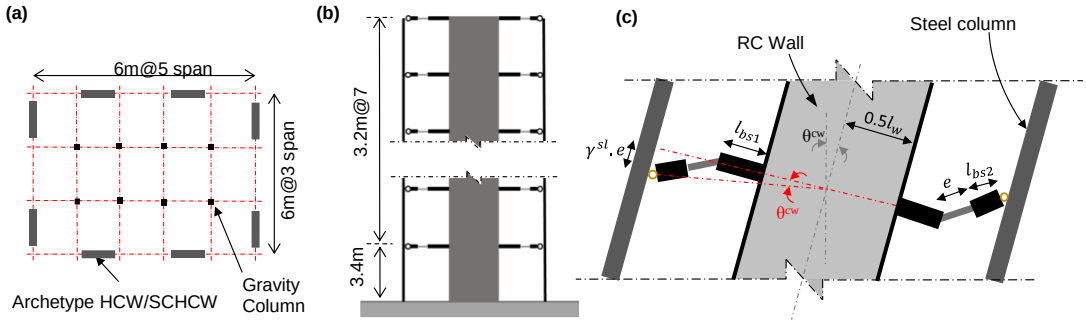

Figure 3. (a) Plan view of the intended eight-story structure, (b) Elevation of the intended eight-story structure, (c) Idealized deformed shape of a SCHW under lateral loading.

The seismic hazard level, system geometry, and coupling ratio are the inputs for the DDBD approach, which should be initially assumed. The performance criteria include the maximum interstory drift limit (θ_c), strain limits for the reinforcement or concrete of the RC wall ($\varepsilon^w_{c,ls}$, and $\varepsilon^w_{s,ls}$ respectively), and the limit state with respect to the links chord rotation (γ^{sl}_{ls}). With respect to the target seismic hazard level, Maximum Credible Earthquake (MCE) and the relevant spectral values in accordance to Eurocode 8 (2004) were considered in this study. γ^{sl}_{ls} was assumed equal to 8% as the rotation limit for short steel links in Eurocode 8 (2004). $\theta_c = 2\%$ and $\varepsilon^w_{s,ls} = 0.05$ (Gogus and Wallace, 2015) were the other performance criteria considered in this study. The interstory drifts relevant to each performance criterion are estimated through the equations suggested by Malla and Wijeyewickrema (2021), and the minimum of them is considered as the interstory drift capacity, θ^{cw}_{cap}. The design displacement profile along the height of the system is subsequently estimated referring to the equations proposed by Priestley *et al.* (2007) and based on θ^{cw}_{cap}. The equivalent SDOF design displacement (Δ_d) and the ductility of the coupled system are evaluated next. It is worth noting that the equations in the DDBD method relating the story drift (θ^{cw}) to the links chord rotation (γ^{sl}) was replaced with the following equation to account for the difference between the behaviour of conventional coupled walls and the intended configuration (Figure 3c).

$$\theta^{cw} = \frac{\gamma^{sl} e}{l_{bs2}+e+l_{bs1}+0.5l_w} \quad (1)$$

where *e* is the length of the links, while l_{bs1} and l_{bs2} are the lengths of the side elements.

When Δ_d is determined, the fundamental period and, consequently, the elastic stiffness of the SDOF system is estimated from the elastic displacement spectrum. The seismic force demand (SDOF base shear) is also evaluated from the inelastic acceleration spectrum. In order to obtain the inelastic acceleration spectrum, a reduction factor calculated based on the ductility of the intended system is applied to the elastic acceleration spectrum (Fajfar, 2000). SDOF base shear is transferred to the system (MDOF) base shear using the modal participation factor, and the seismic force demand in structural members is evaluated accordingly.

It can be assumed that the coupling force is distributed uniformly between the links along the height of the coupled system (El-Tawil et al., 2010). However, Zona *et al.* (2016) suggested that a non-uniform shear distribution and assuming stronger links at the base levels can increase the

ductility of hybrid coupled wall systems with high CRs. Hence, two case study SCHWs with $l_w = 2.5\ m$ (CR=70%) were considered in this study. In one of these case studies (W2.5-U), the SC links activation force was chosen the same at all levels assuming a uniform distribution of coupling force along the height. Conversely, in the other case study system with $l_w = 2.5\ m$ (W2.5-NU), the activation force in the base three levels was increased 20%, while it was decreased 20% for the top three stories. That is, both W2.5-U and W2.5-NU were designed for the same coupling action demand, but different distribution was assumed for the shear force demand on the SC links. Only one case study SCHW with $l_w = 3.2\ m$ (W3.2-U), was designed assuming a uniform distribution of coupling action between the SC links. Table 1 presents a summary of the design outcomes. Four different SC links with the properties listed in Table 2 were implemented in the coupling beams of the case study SCHWs.

Table 3 lists a summary of the key outcomes of the DDBD method. In addition, Figure 4 shows the bilinear prediction of the nonlinear behaviour of W2.5-U (or W2.5-NU) and W3.2-U obtained from the DDBD method. The elastic and inelastic acceleration-displacement spectra for the MCE intensity level are also superimposed in this figure.

	W2.5-U			W2.5-NU			W3.2-U		
Levels	Columns	Side Elements	Links	Columns	Side Elements	Links	Columns	Side Elements	Links
6 to 8	HE300M	IPE550	SCL2	HE300M	IPE450	SCL4	HE300M	IPE550	SCL3
4 to 5	HE400M	IPE550	SCL2	HE400M	IPE550	SCL2	HE400M	IPE550	SCL3
1 to 3	HE400M	IPE550	SCL2	HE400M	IPE550	SCL1	HE400M	IPE550	SCL3

Table 1. Design summary of the steel components of the case study SCHWs

	PT bars	Post-tension force in each bar [kN]	F_{fr} [kN]	F_{act} [kN]	K_{eq} [kN/mm]
SCL1	M16, Grade 10.9	51	110	315	6
SCL2	M16, Grade 10.9	42	100	270	6
SCL3	M16, Grade 10.9	38	85	235	6
SCL4	M16, Grade 10.9	33	70	200	6

Table 2. SC links properties

	Interstory drift capacity	SDOF yield displacement [mm]	SDOF design displacement [mm]	Design ductility	Modal participation factor, Γ	Base shear resistance [kN]
W3.2-U	0.005	62	210	3.4	1.4	1190
W2.5-U/NU	0.006	44	224	5.1	1.36	725

Table 3. Key outcomes of DDBD method for the case study SCHWs

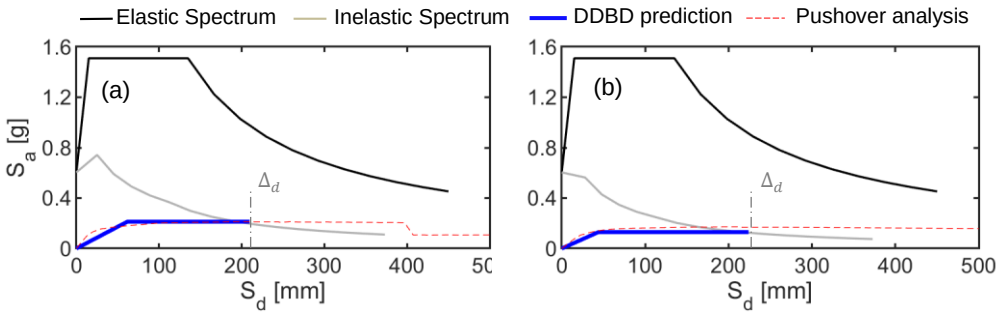

Figure 4. Simplified bilinear behavior of (a) W3.2-U, and (b) W2.5-U under lateral loading predicted through DDBD method

Finite Element models of the case study SCHWs

2D non-linear finite element models of the case study SCHWs were developed in OpenSees (McKenna et al., 2000b). The RC wall was modelled by implementing the Shear-Flexure Interaction Multiple-Vertical-Line-Element-Model (SFI-MVLEM). This modelling approach is based on 2D macroscopic fiber-based model formulation using biaxial constitutive RC panel behaviour (Kolozvari et al., 2015). SFI-MVLEM accounts for the axial force-shear interaction, which is critical for modelling the RC walls subjected to lateral loading. This modelling approach has been calibrated and validated referring to available experimental data, and the modelling parameters obtained from the calibration procedure and suggested by Kolozvari *et al.* (2018) were implemented in this study. The RC wall was discretized to 19 fibers (panels) across its width, which allowed representing the walls' cross-section and different reinforcement arrangements in boundary and web areas. ConcreteCM and Steel02 material models from OpenSees uniaxial materials library were used as the stress-strain relationships for concrete and reinforcement, respectively. In conjunction with Steel02 material model, OpenSees MinMax wrapper was also implemented. The MinMax wrapper reduces the material strength to zero once a maximum or minimum strain is surpassed, and it was used to simulate the tensile fracture or excessive buckling of longitudinal reinforcement bars.

The side elements of the coupling beams were modelled implementing Elastic BeamColumn Elements since they were designed to remain elastic. To account for the elastic shear deformation of the side elements, a zero-length shear spring with a stiffness equal to the shear stiffness of the side elements' cross-section was defined at their connection to the wall. The SC links were modelled using Two-Nodes Link Elements. The mechanical behaviour of Two-Nodes Link Elements is determined by the Unidirectional materials assigned to three springs representing the degrees of freedom of these elements. The Self-Centring Uniaxial material from the OpenSees material Library was the material model assigned to the shear spring of the Two-Nodes Link Elements to represent the flag-shaped shear-deformation behaviour depicted in Figure 2(c).

A distributed plasticity modelling approach was applied to model column elements which allow capturing the axial force-bending moment interaction. Since the gravity system was not modelled, a dummy column was connected to the coupled wall system using rigid-truss elements at every story to account for P-Delta effects imposed to the lateral load-resisting system from the gravity system. The dummy column was modelled with rigid axial elements with a pin support at its base. The ratio of the floor area supported by the gravity system multiplied by the total seismic weight of the floor is considered as the vertical load resisted by the dummy column at each level.

Nonlinear static (pushover) analyses

Nonlinear static (pushover) analyses were performed on the finite element models of the case study SCHWs. The pushover curves are shown in Figure 5. Some critical points (limit states) of the nonlinear behaviour of the case study SCHWs under lateral loading are also highlighted on the curves shown in Figure 5. The limit state with respect to the SC links' behaviour are the roof drifts at which the first and the last link yield and the roof drifts at which the chord rotation of the first and last links exceed $\gamma_{ls}^{sl} = 8\%$. The SC links yield when the shear force demand surpasses the design activation force (F_{act}) reported in Table 2. The onset of concrete crushing (when the confined concrete strain in boundary regions exceeds $\varepsilon_{c,ls}^{w} = 0.005$ (Gogus and Wallace, 2015)) and the first rupture in rebars under tension (when the tensile strain in steel rebars exceeds $\varepsilon_{s,ls}^{w} = 0.05$) are other critical points highlighted in Figure 5.

Figure 5 shows that the activation of SC links occurred before the crushing of concrete or rupture of steel reinforcement, which have been assumed as the key indicators of severe RC wall damage. It should also be noted that the SC links nonlinear behaviour started in all stories before severe damage to the RC wall. Hence the yielding/failure mechanism obtained from pushover analyses for all the case study SCHWs are consistent with what was aimed in the design procedure and satisfies the basic requirement for ductile behaviour.

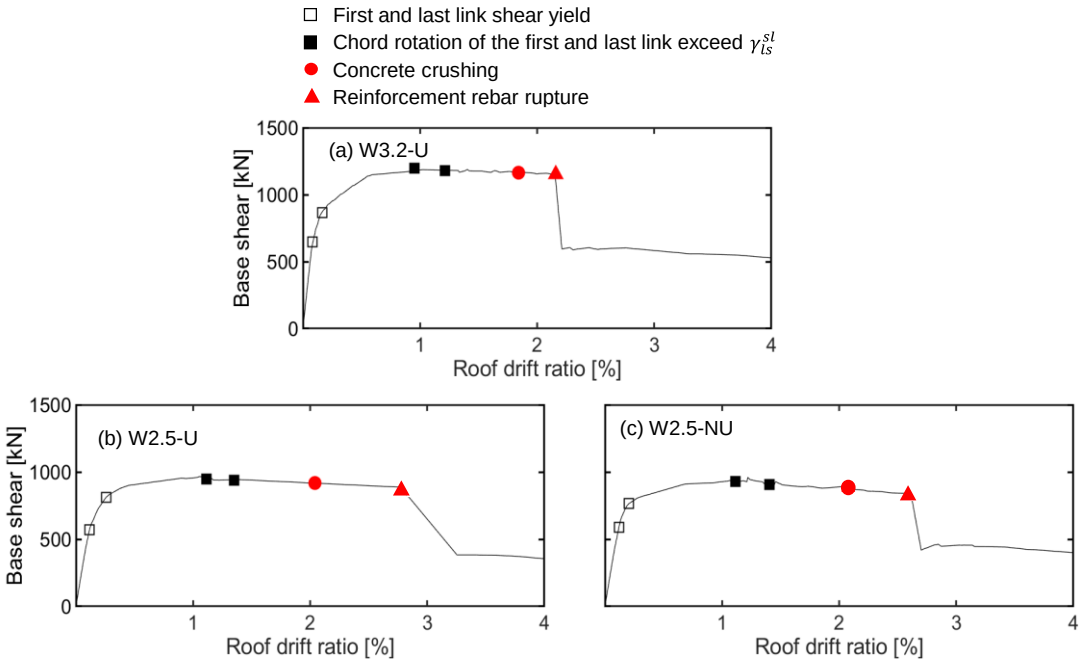

Figure 5. Pushover curves obtained for (a) W3.2-U, (b) W2.5-U, and (c) W2.5-NU

The pushover curves and targeted critical points obtained for W2.5-U and W2.5-NU are similar. That is, the non-uniform distribution of coupling action between links along the height of the W2.5-NU did not notably affect its nonlinear behaviour compared with W2.5-U. The shear force in the SC links at different stories versus the roof drift is also shown in Figure 6 for both W2.5-U and W2.5-NU. It can be inferred from this figure that the SC links at different stories reached their activation force almost at the same time, regardless of how the coupling force was distributed among the shear links along the height.

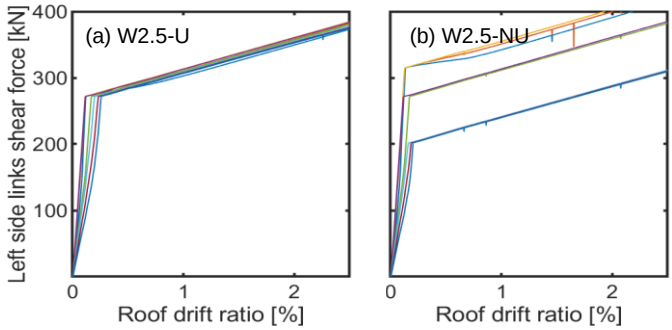

Figure 6. Shear force versus roof drift ratio obtained for the SC links at the left side of the (a) W2.5-U, (b) W2.5-NU

The pushover curves obtained for W3.2-U and W2.5-U are also superimposed in Figure 4. The match between these pushover curves (dashed red line) and the bilinear estimation obtained from the DDBD method (blue filled lines) confirms the sufficiency of DDBD as a simplified method to design hybrid coupled walls and estimate their displacement capacity. The displacement capacity estimated through DDBD was governed by the chord rotation limit state assumed for the links, $\gamma_{ls}^{sl} = 8\%$ in this study. The results of pushover analyses (Figure 5) also confirm that the exceedance of links chord rotation from their capacity proceeded with other targeted failure criteria (rupture of rebars in tension, concrete crushing). Figure 7 represents the DDBD estimation of the interstory drift profiles along the height of the case study SCHWs at their displacement capacity. The interstory drift profiles obtained from the pushover analyses when the chord rotation surpasses $\gamma_{ls}^{sl} = 8\%$ for the first time in one of the SC links (the governing performance criterion marked the displacement capacity in DDBD) are also included in this figure. Figure 7 implied that the profiles obtained from the pushover analyses corroborate those predicted by DDBD method.

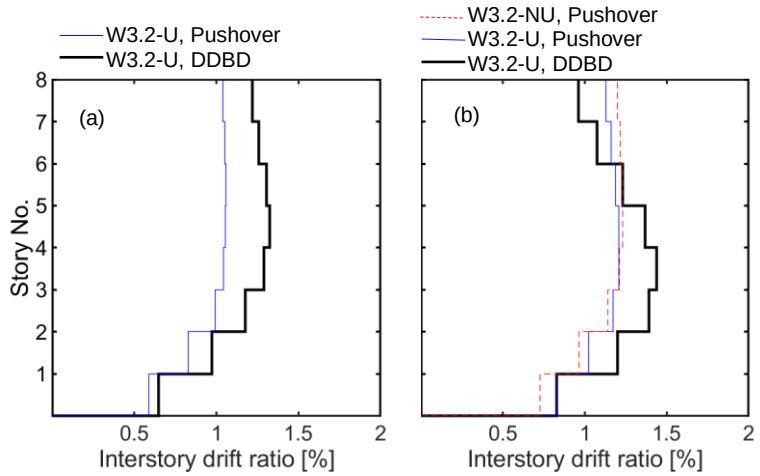

Figure 7. Interstory drift profile along the height of (a) W3.2-U, and (b) W2.5-U/W2.5-NU at their displacement capacity obtained from DDBD.

Nonlinear dynamic analyses

The seismic performance of the case study SCHWs was also examined by performing nonlinear dynamic (time-history) analyses using OpenSees structural simulation platform (McKenna et al., 2000a). In these analyses, the finite element models prepared for the case study SCHWs were subjected to several ground motions scaled to increasing intensity levels (Vamvatsikos and Cornell, 2002). The 22 pairs of far-field ground motion records suggested by FEMA P695 (FEMA, 2009) were used in this study. The spectral acceleration at the fundamental period, $S_a(T_1)$, was selected as the Intensity Measure (IM). The fundamental periods of the case study SCHWs were evaluated very close, and the average of the values obtained for the three case study SCHWs, $T_{1,ave}$*=0.9 sec*, was considered as the reference fundamental period for assessing IMs. Maximum Credible Earthquake (MCE) intensity level was considered as the reference intensity levels. MCE intensity level was obtained equal to 1g from the Eurocode 8 (EN1998-1, 2004) spectrum at $T_{1,ave}$=0.9 sec.

Figure 8(a) shows the response of the case study SCHWs in terms of the roof drift ratio to a ground motion record recorded during the Northridge Earthquake and scaled to MCE intensity level. The negligible residual roof drifts at the end of the analyses highlight the self-cantering capability of the coupled wall configuration proposed in this study. The chord rotation-shear force response of the left link at the 4th story of the case study SCHWs is also shown in Figure 8(b). This figure illustrates that the earthquake-induced chord rotation of the SC links was fully retrieved.

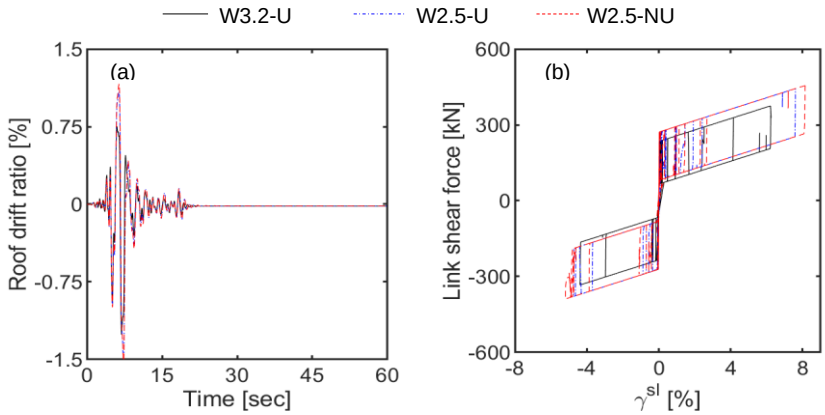

Figure 8. (a) Roof drift time history, and (b) shear force-chord rotation response of the 4th story left link for the case study SCHWs

Figure 9 shows the maximum interstory drift at the end of analyses (the maximum residual interstory drift) as an indicator of the SC capability of the case study SCHWs. The median of the

results obtained under 44 ground motion records for each IM is represented with solid lines, and the shaded areas represent the variation of the results between 16% and 84% fractiles.

The first damage state (DS) threshold of 0.2% (DS1) suggested by FEMA P-58 (2018) for the residual interstory drifts is also superimposed in**Error! Reference source not found.** Figure 9. This limit state represents the maximum interstory drift at which no structural realignment is required for structural stability, while non-structural and mechanical components may need to be repaired. As it can be inferred from this figure, the DS1 limit was not exceeded at MCE intensity level (IM=1g) for none of the case study SCHWs. These results identify the efficiency of the friction-based SC links in limiting the residual deformation and, consequently, the superior repairability and seismic resilience of SCHWs.

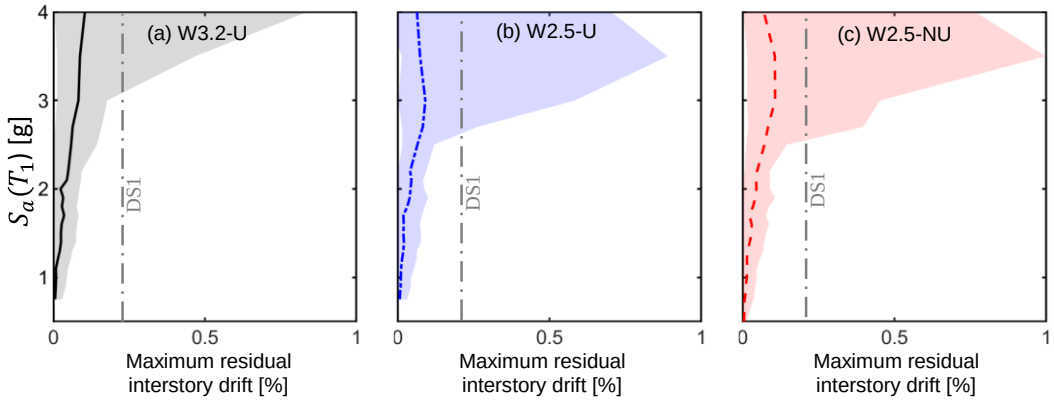

Figure 9. Maximum residual interstory drift of (a) W3.2-U, (b) W2.5-U, and (c) W2.5-NU

Conclusions

This paper presented the results of a numerical study about the seismic performance of self-centring hybrid coupled walls (SCHWs), which the efficiency of SCHWs in eliminating earthquake-induced residual deformations. The design procedure implemented in this study was also proved to be efficient to ensure the SC links are the first elements yield under lateral loading and start dissipating energy before excessive damage to other components. In addition, the accuracy of the displacement capacity estimated by the direct displacement-based design (DDBD) approach for the case study SCHWs was examined and approved in comparison with the results of the nonlinear static analyses. The results of nonlinear dynamic analyses confirmed the efficiency of using the proposed SC links in minimizing the earthquake-induced residual deformations and the supremacy of SCHWs as seismic-resilient lateral load-resisting systems.

Acknowledgements

This research was supported by the European Union's Horizon 2020 research and innovation program under grant agreement No. 101027745 (Marie Sklodowska-Curie Research Grant Scheme H2020-MSCA-IF-2020: Self-Centring Earthquake-Resilient Hybrid Steel-Concrete Shear Walls with Rocking Beams - SC-HYBWalls). The Authors also acknowledge the support from the Royal Society - International Exchange programme under the grant agreement IES\R3\213175.

References

FEMA P58 .2018. Seismic Performance Assessment of Buildings, FEMA P58. Washington, D.C.: Federal Emergency Management Agency.

DAS, R., ZONA, A., VANDOREN, B. & DEGÉE, H. 2018. Optimizing the coupling ratio of seismic resistant HCW systems with shear links. *Journal of Constructional Steel Research,* 147**,** 393-407.

DENG, K., PAN, P. & WU, S. 2016. Experimental study on a self-centering coupling beam eliminating the beam elongation effect. *The Structural Design of Tall and Special Buildings,* 25**,** 265-277.

EL-TAWIL, S., HARRIES, K. A., FORTNEY, P. J., SHAHROOZ, B. M. & KURAMA, Y. 2010. Seismic Design of Hybrid Coupled Wall Systems: State of the Art. *Journal of Structural Engineering,* 136**,** 755-769.

EN1998-1. 2004. *Eurocode 8: Design of structures for earthquake resistance* Brussels.

FAJFAR, P. 2000. A Nonlinear Analysis Method for Performance-Based Seismic Design. *Earthquake Spectra,* 16**,** 573 - 592.

FEMA 2009. Quantification of building seismic performance factors. *FEMA P695.* Washington, DC: FEMA.

GOGUS, A. & WALLACE, J. W. 2015. Seismic Safety Evaluation of Reinforced Concrete Walls through FEMA P695 Methodology. *Journal of Structural Engineering,* 141**,** 04015002.

HUANG, X. & WANG, Y. 2021. Development and modelling of new friction damped self-centring link for coupled wall systems. *Engineering Structures,* 239**,** 112365.

KAM, W. Y. & PAMPANIN, S. 2011. The seismic performance of RC buildings in the 22 February 2011 Christchurch earthquake. *Structural Concrete,* 12**,** 223-233.

KOLOZVARI, K., ORAKCAL, K. & WALLACE JOHN, W. 2015. Modeling of Cyclic Shear-Flexure Interaction in Reinforced Concrete Structural Walls. I: Theory. *Journal of Structural Engineering,* 141**,** 04014135.

KOLOZVARI, K., TERZIC, V., MILLER, R. & SALDANA, D. 2018. Assessment of dynamic behavior and seismic performance of a high-rise rc coupled wall building. *Engineering Structures,* 176**,** 606-620.

MALLA, N. & WIJEYEWICKREMA, A. C. 2021. Direct displacement-based design of coupled walls with steel shear link coupling beams. *Structures,* 34**,** 2746-2764.

MCKENNA, F., FENVES, G., SCOTT, M. & JEREMIC, B. 2000a. Open System for Earthquake Engineering Simulation (OpenSees). UC Berkeley (CA): Pacific Earthquake Engineering Research Center.

MCKENNA, F., GL, G. F., SCOTT, M. & JEREMIC, B. 2000b. Open System for Earthquake Engineering Simulation (OpenSees). C Berkeley (CA): Pacific Earthquake Engineering Research Center.

PRIESTLEY, M., CALVI, G. & KOWALSKY, M. Direct displacement-based seismic design of structures. NZSEE conference, 2007. Citeseer, 1-23.

RICLES, J. M., SAUSE, R., PENG, S. W. & LU, L. W. 2002. Experimental evaluation of earthquake resistant posttensioned steel connections. *Journal of Structural Engineering,* 128**,** 850-859.

SHAHROOZ, B. M., REMMETTER, M. E. & QIN, F. 1993. Seismic design and performance of composite coupled walls. *Journal of Structural Engineering (United States),* 119**,** 3291-3309.

VAMVATSIKOS, D. & CORNELL, C. A. 2002. Incremental dynamic analysis. *Earthquake Engineering & Structural Dynamics,* 31**,** 491-514.

WALLACE, J. W., MASSONE, L. M., BONELLI, P., DRAGOVICH, J., LAGOS, R., LÜDERS, C. & MOEHLE, J. 2012. Damage and implications for seismic design of RC structural wall buildings. *Earthquake Spectra,* 28**,** S281-S299.

WANG, Y. 2008. Lessons learned from the “5.12” Wenchuan Earthquake: evaluation of earthquake performance objectives and the importance of seismic conceptual design principles. *Earthquake Engineering and Engineering Vibration,* 7**,** 255-262.

WELDON, B. D. & KURAMA, Y. C. 2010. Experimental evaluation of posttensioned precast concrete coupling beams. *Journal of Structural Engineering,* 136**,** 1066-1077.

WESTENENK, B., DE LA LLERA, J. C., BESA, J. J., JÜNEMANN, R., MOEHLE, J., LÜDERS, C., INAUDI, J. A., ELWOOD, K. J. & HWANG, S.-J. 2012. Response of Reinforced Concrete Buildings in Concepción during the Maule Earthquake. *Earthquake Spectra,* 28**,** 257-280.

ZAREIAN, M. S., ESFAHANI, M. R. & HOSSEINI, A. 2020. Experimental evaluation of self-centering hybrid coupled wall subassemblies with friction dampers. *Engineering Structures,* 214**,** 110644.

ZONA, A., BONI, P., DEGÉE, H., LEONI, G., VARELIS, G., SALVATORE, W., BRAHAM, C., HOFFMEISTER, B., BOGDAN, T., DALL’ASTA, A., MORELLI, F., TSINTZOS, P., BIGELOW, H., MEDICI, E., GALAZZI, A. & KARAMANOS, S. 2015. *Innovative hybrid and composite steel-concrete structural solutions for building in seismic area (INNO-HYCO) : final report*, Publications Office.

ZONA, A., DEGÉE, H., LEONI, G. & DALL'ASTA, A. 2016. Ductile design of innovative steel and concrete hybrid coupled walls. *Journal of Constructional Steel Research,* 117**,** 204-213.